PERGAMON

Computers & Geosciences 25 (1999) 383–394

COMPUTERS & GEOSCIENCES

Thin-plate and thin-shell finite-element programs for forward dynamic modeling of plate deformation and faulting☆

Peter Bird *

Department of Earth and Space Sciences, University of California, Los Angeles, CA 90095-1567, USA

Received 27 May 1998; received in revised form 8 July 1998; accepted 8 July 1998

Abstract

Experiments on deformation of the lithosphere can be performed only in computers. Finite-element codes are best because they can represent lateral strength variations, including faults. Although variations of temperature, strength, and density in the lithosphere must be represented in three dimensions, it is usually sufficient to parameterize the velocity field in two dimensions, giving 'thin-plate' or 'thin-shell' codes. Four such freeware codes (LARAMY, FAULTS, PLATES and SHELLS) are offered at `ftp://element.ess.ucla.edu`. Their capabilities include local neotectonic problems with many faults, global neotectonic problems with many plates and finite strain problems with crust/mantle detachment; the only capability not yet available is finite strain with discrete faults of large offset. Model predictions include velocities, fault-slip rates, anelastic strain rates and vertically integrated stresses, which can be tested by comparison with data from geologic mapping, seismology and geodesy. © 1999 Elsevier Science Ltd. All rights reserved.

Keywords: Tectonophysics; Neotectonics; Lithosphere; Plate tectonics

1. Introduction

Structural geology and tectonophysics have been slow to take their places among the rigorous, quantitative sciences. The first problem, the lack of a central paradigm, was solved by the plate tectonic revolution. The study of continental-scale processes benefitted the most from plate tectonic theory, because it provides the necessary boundary conditions. The second problem, however, is the difficulty of conducting experiments. Whereas small volumes of rock can be heated and compressed in the laboratory, experiments on the movement and deformation of whole lithospheric plates can only be performed in computers.

Such numerical experiments are often referred to as 'forward' or 'dynamic' models, in which one solves the equations of stress equilibrium (conservation of momentum) and conservation of mass with some assumed rheologies and densities in order to predict velocities, stresses and strain rates. These should be distinguished from 'inverse' or 'least-squares' models in which a smooth velocity field is fit to some observations about fault slip and/or strain rate without regard for dynamic equilibrium. (The author is also developing such a program, named RESTORE, but it will be the subject of a future paper.)

In choosing between possible formalisms for dynamic models, it is important to remember that the deformation mechanisms which determine rock

☆ Code available at http://element.ess.ucla.edu

* Tel.: +1-310-825-1126; fax: +1-310-825-2779; e-mail: pbird@ess.ucla.edu

PII: S0098-3004(98)00142-3

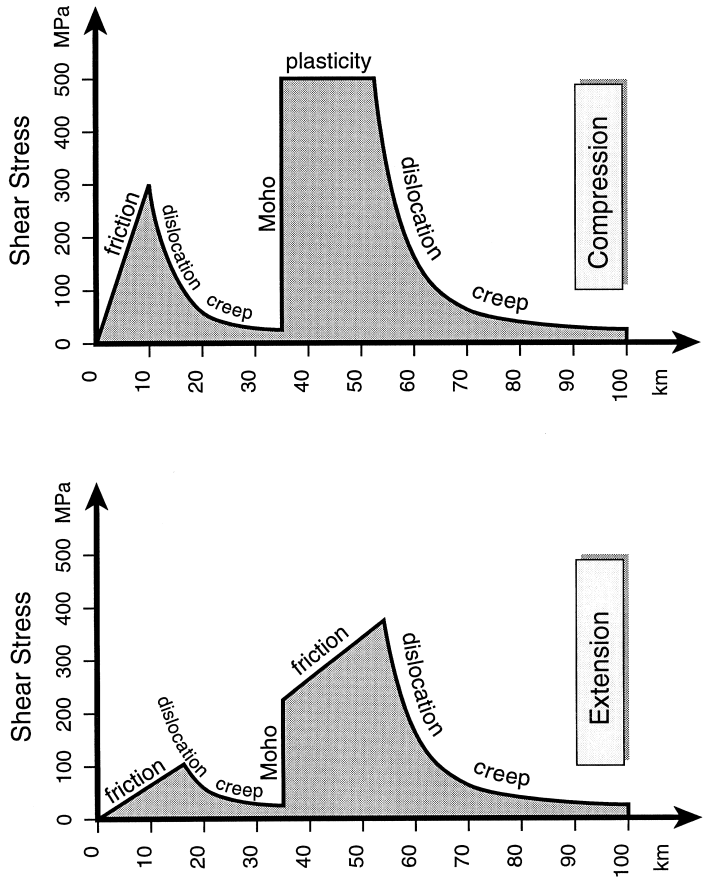

Fig. 1. Typical vertical distribution of maximum shear stress in continental lithosphere undergoing compressional (right) or extensional (left) strain at 1×10^{-15}/s. Friction controls level of shear stress in upper part of crust and sometimes in mantle lithosphere; then, below brittle/ductile transition, shear stress is controlled by thermally-activated dislocation creep.

strength (friction and dislocation creep) are nonlinear. This rules out most analytical and spectral methods for solving the governing equations. Among the numerical methods, finite-element has a strong advantage over finite-difference because it does not require that lateral transitions in material properties be spread over a number of grid points. Also, finite-element methods can represent faults of arbitrary shape.

Within the lithosphere, the vertical gradients of temperature and pressure give rise to at least one brittle/ductile transition, which is the transition from friction to dislocation creep as the dominant or stress-regulating strain mechanism. In continents, there may be one such transition in the crust and a second in the mantle lithosphere (Fig. 1). An accurate representation of lithospheric strength requires three-dimensional volume integrals. However, in many problems it is a good approximation to say that horizontal velocity components are independent of depth. This approximation is called the 'thin-plate' or 'thin-shell' modeling method and it gives a critical reduction in computation cost over fully three-dimensional finite-element grids.

The authors methods are two-dimensional in the sense that only the horizontal components of the momentum equation are solved (in vertically-integrated weak form) using 2D finite-element grids and only the horizontal components of velocity are predicted. The vertical (radial) component of the momentum equation is represented by the isostatic approximation. Therefore, vertical normal stress at any point is assumed equal to the weight of overburden per unit area. (Bending stresses such as those occurring in the outer rises of subduction zones are not represented.) On the other hand, the methods of the author are three-dimensional in the sense that volume integrals of density and strength are performed numerically in a lithosphere model with laterally-varying crust and mantle-lithosphere layer thicknesses, laterally-varying heat flow and laterally-varying topography. Furthermore, they are programmed to compute and apply horizontal tractions to the base of the litho-

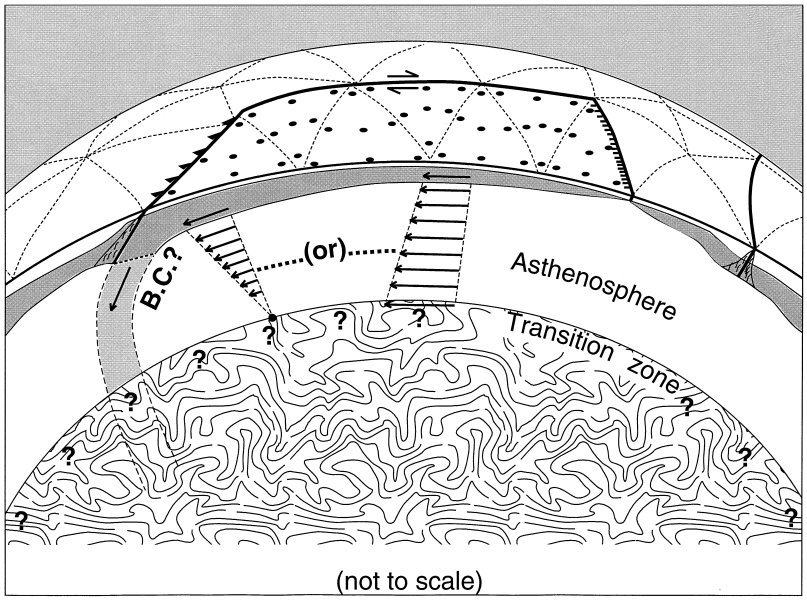

Fig. 2. Cartoon of the geometry assumed in program SHELLS. Crust (white) is bonded to the mantle lithosphere (shaded) and their joint strength is represented by 2D grid of spherical triangles on surface. Within each triangle, vertical integrals of strength are performed at 7 G integration points (black dots). Fault elements are used to represent plate boundaries. Because subducting slabs deeper than 100 km are not included in model, their 'cut' ends require boundary conditions (either velocity or traction specified). Whether lower mantle is assumed to be fast-moving or sluggish, velocity differences between lower mantle and lithosphere cause simple shear in asthenosphere, which applies horizontal shear tractions to base of model.

sphere if it shears over a deeper layer (Fig. 2). Thus, they might be called '$2\frac{1}{2}$-dimensional' methods.

2. Assumptions and approximations

1. Geometry: depending on the program, the surface of the planet s approximated as (locally) flat or as spherical. Gravity is assumed to be constant and vertical. Topography is considered as a source of stress, but the 2D finite element grid is everywhere at sea level.
2. Creeping flow (quasi-steady state): because the time scale we model is much larger than that of the earthquake cycle, all accelerations except gravity are ignored.
3. Anelastic rheology: in a quasi-steady state with constant boundary conditions, elasticity contributes a negligible fraction of the strain-rate in viscoelastic solutions (Bird and Kong, 1994). Elastic strain is entirely neglected to eliminate arbitrary initial conditions and time-steps.
4. No flexural strength: no vertical shear traction is assumed on vertical planes and it is assumed that vertical normal stress is therefore lithostatic at all points. (Also, most parts of most models will be designed to be isostatic, but this is not a constraint of the method. If the density structure implies anomalous tractions at the base of the model, such tractions will be properly considered in the momentum balance.)
5. Thin plate or shell: the horizontal components of the momentum equation are vertically integrated through the plate and solved in a 'weak' or 'Galerkin' form, using a self-consistent set of test functions.
6. Constant thermal properties: constant thermal conductivity and heat productivity in all parts of crust are assumed, with (distinct) constant properties in all mantle lithosphere.
7. Incompressibility (consistent with neglect of elastic strain).
8. Steady-state, vertical heat conduction: in all of the authors programs but one, the geotherm is assumed to be in steady-state and to depend only on heat flow and thermal properties. (However, in the time-

Table 1
Comparison of freeware programs offered here

Program	Application	Refs.	New features	Limitations
LARAMY	western United States	Bird (1988, 1989, 1992)	method for convergence; two-layer grid (crust, mantle lithosphere); finite strain	flat-Earth; no faults in interior
FAULTS	California	Bird and Kong (1994)	fault elements	one-layer (crust); flat-Earth; neotectonic
PLATES	Alaska	Bird (1996)	strength of crust and mantle lithosphere combined (one-layer)	neotectonic; flat-Earth; no detachment of crust from mantle lithosphere
SHELLS	Asia	Kong (1995) and Kong and Bird (1995, 1996)	spherical-shell	neotectonic; no detachment of crust from mantle lithosphere
SHELLS	Earth	Bird (1998)	whole-Earth	neotectonic; no detachment of crust from mantle lithosphere

dependent finite-strain program, the geotherms evolve over time.)

3. Differences between programs

The author offers four variants of this method as freeware to the community, in Fortran 77 programs LARAMY, FAULTS, PLATES, and SHELLS. All are available by anonymous FTP from `element.ess.ucla.edu`. These codes can be compiled for use on almost any operating system.

LARAMY is the only program which computes finite strain over time, and it offers the possibility of horizontal crust/mantle detachment in continents; however, it is unable to incorporate internal faults. The other three codes include faults, but are only neotectonic, meaning that they represent the kinematics and balance of forces at only one epoch in geologic time (usually, but not necessarily, the present). A detailed comparison of the authors programs, with references and examples, is presented in Table 1.

It may also be useful to contrast these programs with those developed by others. There are pronounced differences in three aspects: (i) rheology of the continuum; (ii) representation of faults and (iii) representation of sphericity.

A large number of modelers have treated plate interiors as elastic (e.g. Richardson, 1978; Richardson et al., 1979; Solomon et al., 1980; Kasapoglu and Toksöz, 1983; Richardson and Reding, 1991; Grunthal and Stromeyer, 1992; Grindlay and Fox, 1993; Coblentz and Richardson, 1996; Lundgren and Russo, 1996; Peltzer and Saucier, 1996). However, in the absence of cohesion (and the longevity of cohesion over geologic time is dubious), any amount of deviatoric stress initiates frictional failure which propagates downward from the surface as stress increases and also creep failure which propagates upward from the plate bottom as time passes. While plate interiors under very low deviatoric stress for short times may retain an elastic core, regions with 'interesting' rates of deformation will not. Elasticity is incompatible with any level of intraplate seismicity, but intraplate seismicity is common. It can also be observed that a purely elastic planet would not have plates because it would not have an asthenosphere. Thus, elasticity is a very crude approximation, which is least successful where high stresses act for long times. Linear or 'Newtonian' viscosity has also been used (Richardson and Cox, 1984) because of its convenient linearity, but unfortunately there is little laboratory support for linear viscosity of Earth materials. England and co-workers (e.g. England and Houseman, 1985, 1986, 1989; England et al., 1985; England and Searle, 1986; Houseman and England, 1986, 1993; Sonder et al., 1986) represent the strength of the lithosphere by a power-law, which is intended to approximate the combined strengths of the creeping and the faulting layers. However, their symmetrical formula does not represent the greater strength of the lithosphere in compression and its relative weakness in extension (this effect introduces a factor of 4.7 in frictional strength when friction is 0.85). Other approximations have included elastoplasticity (Wang et al., 1997) and nonlinear viscoplasticity (e.g. Vilotte et al., 1982, 1984, 1985). Apparently, Wang et al. (1995) are the only others to have programmed the asymmetric Coulomb friction law. The authors programs are currently the only ones which include a transition from

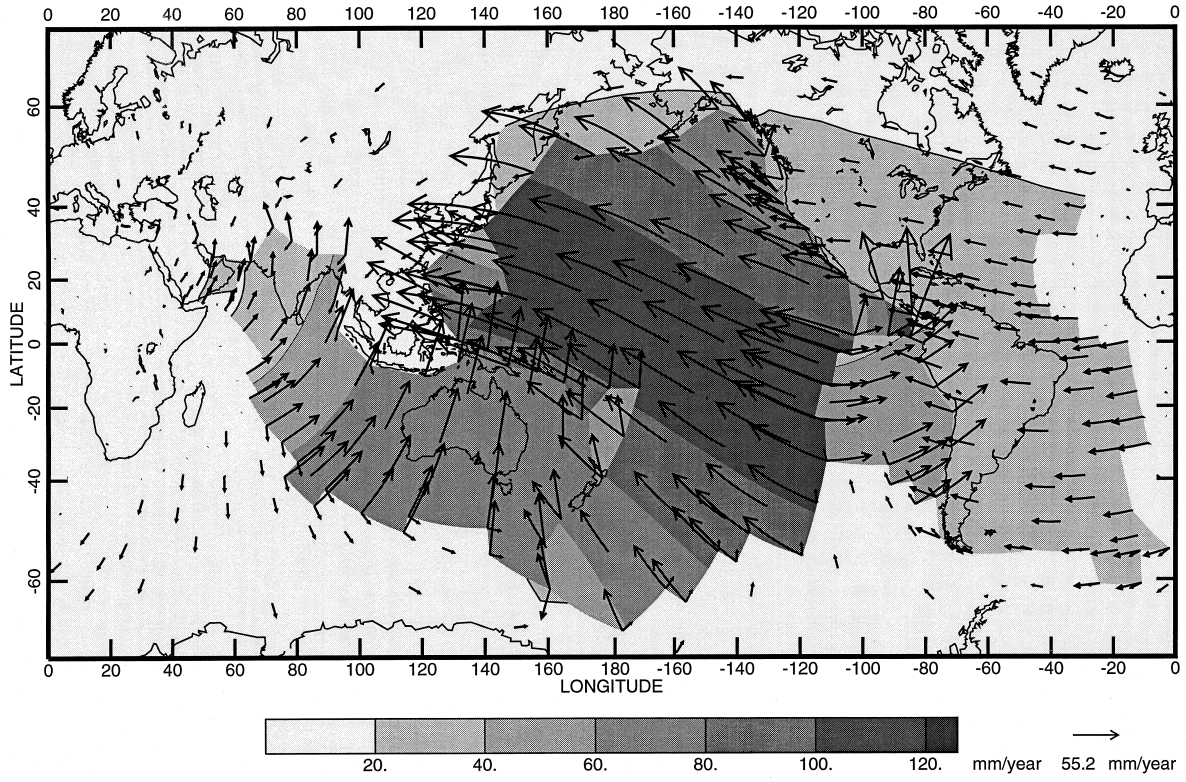

Fig. 3. Mercator projection of velocities from global spherical model 98027, based on model 97001 of Bird (1998). Reference frame is Africa-fixed. Velocity is discontinuous at plate edges, which were represented by fault elements (not shown). Velocity variations within plates are primarily due to rotation on sphere, not to strain. Flow in this model is driven by combination of topography, slab pull, and active drag beneath continents. Except in Cocos plate, its predictions of velocity and stress are reasonably accurate. Computed with SHELLS and plotted with OrbMapAI.

Coulomb friction to nonlinear dislocation creep at variable depth depending upon the strain rates in the solution.

Most of the programs referenced previously (and the authors program LARAMY) have no provision for faults. Some early workers (e.g. Richardson et al., 1979; Bird and Piper, 1980; Solomon et al., 1980) tried to approximate faults as linear weak zones of continuum elements; we quickly found that this leads to a number of artifacts. True faults (velocity discontinuities) were first introduced into thin-plate models by Kasapoglu and Toksöz (1983) who assigned them a coefficient of friction and then iterated the solutions to see if they would slip. A few programs (e.g. Lundgren and Russo, 1996; Peltzer and Saucier, 1996) have incorporated faults by specifying their slip rates, rather than deriving them self-consistently from the solutions. This may force the velocity fields to look more realistic, but only at the expense of introducing large fictitious forces along faults; it is considered that these belong to a different class of inverse modeling programs which are not attempting dynamic self-consistency. The authors programs FAULTS, PLATES and SHELLS have an advantage in having special fault elements which incorporate the strengths of both the frictional and the creeping layers, including the effects of variable normal stress on strike-slip faults.

It is also true that most programs prior to SHELLS have assumed a flat Earth. Richardson and co-workers pioneered modeling on the sphere, by the simple expedient of treating it as locally flat within each element, then assembling element strengths in spherical coordinates. Apparently, the inverse modeling program of Peltzer and Saucier (1996) is the only code besides our SHELLS to use actual spherical-shell elements. Shell elements should give better accuracy for the same number of nodes.

4. The modeling cycle

The following is a suggested outline for the application of one of the authors programs to modeling a specific region. The discussion is based on program SHELLS; small differences in approach when using the other programs will be noted parenthetically. Fuller discussions of the use of each program are available as individual 'Read_Me' text files on the FTP site.

1. Create a finite-element grid. This is done by running interactive utility program OrbWeave. (For FAULTS or PLATES, the corresponding grid editor program is DrawGrid; program LARAMY creates its own grids.) OrbWeave was written in Microsoft® BASIC 7.0 and compiled for DOS® (or Windows®, or any other O/S that emulates DOS). Notice that you are permitted to load a base map (a file of digitized line segments) for location reference; you can use the authors program Digitize (for DOS) with a serial-port digitizer to create your own base map files in flat-Earth (x, y) coordinates and the authors utility program Projector to convert these to (*longitude*, *latitude*). Nodes and elements can be entered singly, or as regions of uniform element size. Grids which will contain faults are initially created as continuous, and then faults are 'cut' along element sides; each fault must be assigned a dip angle. Commands within OrbWeave (and DrawGrid) are available to test the grid for topological errors (which may occur when grids created by other programs, or by hand, are imported.)
2. Renumber the nodes of the finite-element grid for minimum bandwidth. The authors Fortran 77 utility program OrbNumbr will perform this necessary step as a batch job on any computer system. (For FAULTS or PLATES, the corresponding utility is Number; LARAMY grids do not require renumbering.)
3. Assign nodal data for each node of the finite element grid. Following each node number, with its longitude and latitude (or (x, y) in the case of FAULTS and PLATES), you must supply: elevation, heat-flow, crustal thickness and mantle-lithosphere thickness (the last is not used by FAULTS). (Note that OrbWeave and DrawGrid initialize these values as zero when new nodes are created, but retain data attached to old nodes which are edited. OrbNumbr and Number also retain nodal data when they renumber nodes.) Although it is not mathematically required, it is *strongly suggested* that you balance these input values to produce a model which is everywhere isostatic with respect to mid-ocean spreading rises. Otherwise, a nonzero anomaly in the vertical normal stress at the base of the lithosphere will be computed by SHELLS (or FAULTS or PLATES) and will enter the balance of horizontal forces in two ways: (i) wherever the base of the lithosphere is not horizontal, it will produce a horizontal boundary traction component and (ii) wherever lithostatic load is computed as the constant term in horizontal normal stresses (before the addition or subtraction of deviatoric stresses) it will affect the plate strength. In order to achieve isostasy, it is suggested that you provide no more than elevation and heat-flow and let (at least) the layer thicknesses be computed by the authors Fortran 77 utility program OrbData. (The corresponding utility for PLATES is AK_nodes.) OrbData uses an iterative computation which will usually succeed in finding an isostatic balance for each node.
4. Check and edit the nodal data. Return to the interactive editor OrbWeave and use command 'Q' to display your nodal data. The same command allows you to modify any value by clicking the mouse on a node and then typing a correction. (Unfortunately, DrawGrid does not have this feature.)
5. Plot maps of your nodal data, to check for errors. First, notice that lines 33 and higher of the parameter input file are not read by SHELLS (or the other 3 F–E programs) and are reserved for control of graphics output. Alter these latter lines (from the sample file i98027.in, provided) to control which plots will be produced, at what scale, with what center point and what contour interval, etc. Then, compile Fortran 77 graphics program OrbMapAI (or, use the executable provided for Windows 95® or Windows NT®). (The corresponding graphics programs for use with FAULTS, PLATES and LARAMY are Faults2AI, Plates2AI and Laramy2AI, respectively.) If you compile on a Unix system, you will probably need compiler switch '-qnoescape' (or something similar) to guarantee that character '\' is treated as a simple backslash and not as the escape character. OrbMapAI will produce text files of PostScript® in the Adobe Illustrator® dialect. Download these files (as ASCII text) to a Windows® PC or Macintosh® running Adobe Illustrator® version 4 or 7, from which they can be viewed, edited and printed.
6. Decide whether models will be subjected to horizontal tractions on the base of the lithosphere. Each of the four codes contains the option for 'soft' linkage between the surface velocities which are to be calculated and some deeper flow field which is assumed and held constant. LARAMY always couples crustal flow to mantle lithosphere flow across a shear zone in the lower crust and

couples both layers of the lithosphere to horizontally-subducting oceanic slabs where and when they were present. FAULTS can couple crustal flow to assumed mantle lithosphere flow across a shear zone in the lower crust. PLATES can couple lithosphere flow (crust and mantle lithosphere moving as a unit) to subducting oceanic slabs in a forearc region of contact. SHELLS can couple lithosphere flow to assumed lower-mantle flow across a shear zone in the asthenosphere (Fig. 2). For specific applications other than those we have published (Table 1), it may be necessary to modify portions of the code which describe the kinematics of the assumed flow of the deeper layer. Of course, if no basal shear tractions are wanted, then the input parameter giving the maximum value of such shear traction can be set to zero, in which case the pattern of the deeper flow becomes irrelevant.

7. Compile the finite-element program with a Fortran 77 (or Fortran 90) compiler. Notice that you (or your computer center) must supply the subroutines to solve the large banded linear systems of equations that result from any finite-element problem. In SHELLS, we used routines DGBF and DGBS from the IBM® Engineering Sciences Subroutine Library®. If you do not have access to this, you will have to substitute other routines. To make the substitution as easy as possible, we have isolated the calls to DGBF and DGBS in a short subroutine SOLVER, which is the main thing you will need to modify. Unfortunately, a different linear-system solver for banded matrices may expect a different storage scheme for the coefficient matrix. In order to make such changes possible, we have dimensioned the compressed banded coefficient matrix (STIFF or K) as a *one*-subscript vector of great length, and then used statement function INDEXK to compute the storage location in this long vector from the logical row and column number of the virtual full matrix. Therefore, you can change storage schemes by changing statement function INDEXK, in every routine in which it appears. As a final change, you may have to adjust the formula in subroutine KSIZE of SHELLS, whose function is to make sure that the dimensioned size of the workspace is large enough for the problem at hand.
8. Run the finite element program to get a list of boundary nodes, which require boundary conditions. SHELLS (or FAULTS or PLATES) will stop when boundary conditions are not found, but will first provide a list of boundary nodes in order. Use a text editor to extract this last table from the output and make it the skeleton of your boundary-conditions input file.
9. Select boundary conditions for each node where required. If your model is regional and has a side boundary, this list should proceed in counterclockwise order around the boundary. You need to be aware of some subtleties of the topology. First, if you have placed fault elements along the perimeter of your model, then the boundary nodes are the ones *outside* the fault, and they belong the *adjacent* plate, not the one whose volume you are modeling. Therefore, assign them the velocities of the neighboring plate(s). Second, wherever there are faults along the boundary, there is the possibility that they connect in triple-junctions to additional faults which are outside the perimeter of the model. That is, at every end of every boundary fault element, there is a chance of a change in the name and Euler pole of the neighboring plate. For this reason, the grid will have *two distinct* nodes on the outside of the boundary at each point where two boundary faults meet. Both require boundary conditions. The first one listed belongs to the boundary fault which comes first as you go counterclockwise around the boundary. On the other hand, your model may cover the whole globe and have no side boundaries. In this case, SHELLS will search for 'subduction zones', which it will identify as faults of less than a critical dip angle. Subduction zones require a boundary condition for the subducting plate *only*, because the subducting slab is truncated at 100 km depth and not included in the model (Fig. 2). (It is also theoretically possible to do a global model with no subduction zones and thus no boundary conditions, but this has never been tried.) For each node in the boundary list, you may choose to leave it 'free' (subject only to lithostatic normal traction), to constrain one component of velocity, or to constrain both components.
10. Edit the parameter input file. Either accept or modify the parameters of i98027.in to set the rheologic and other constants you want. Use a consistent system of units; SI is suggested. For the first line, choose a title to describe this particular experiment; it will be passed through to output files and plots automatically. Be careful when changing the density or geothermal parameters (radioactivity, conductivity, thermal expansion): you are certainly free to do so, but any change in these particular parameters will cause your model to go out of isostatic balance, thus requiring you to go back to step #3 and recompute layer thicknesses.
11. Run a simulation experiment. Your output will appear as follows: Fortran unit 6 will have text output, including echoed input and output tables. Fortran unit 9 will have nodal velocity vectors. Fortran unit 10 will have the boundary nodal

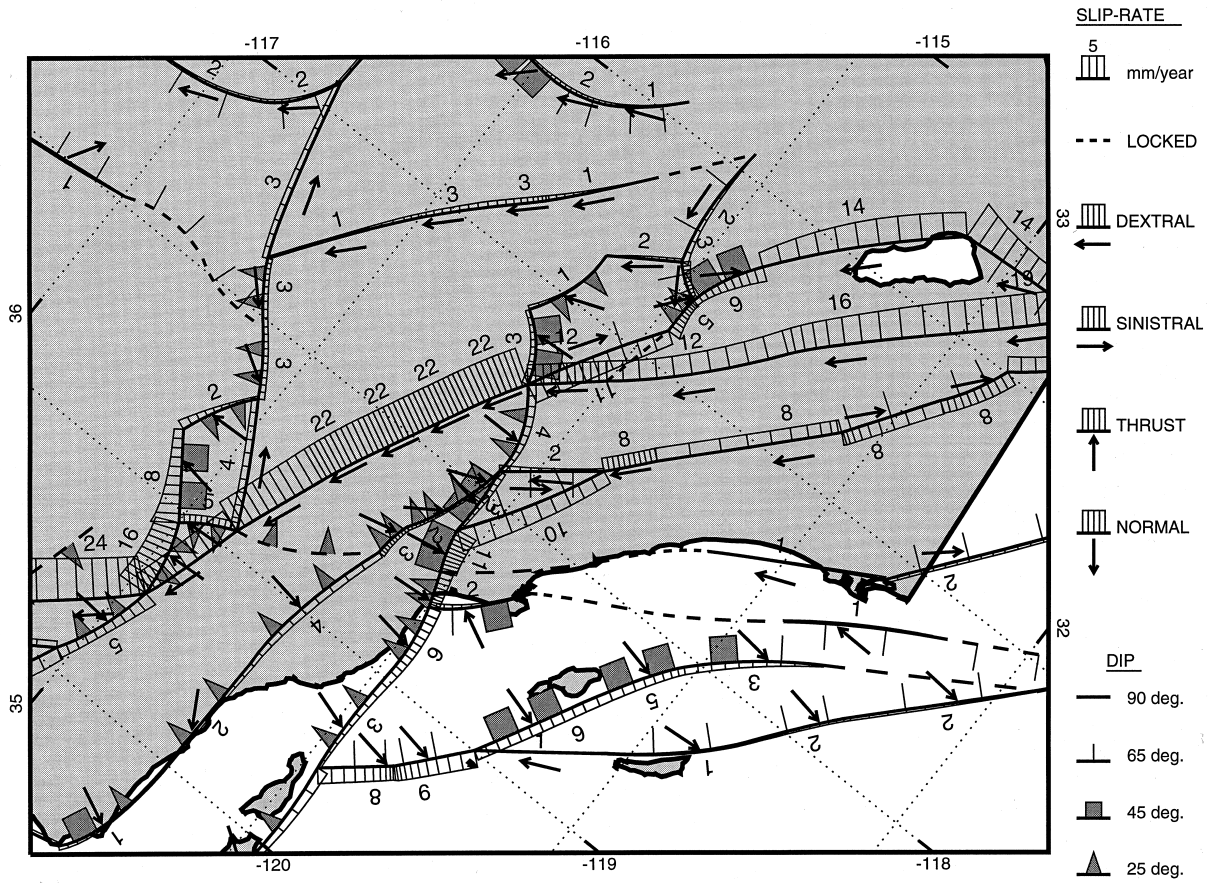

Fig. 4. Detail of predicted fault slip rates in southern California from model 98C813, based on best model found by Bird and Kong (1994). Width of ribbon plotted beside fault is proportional to long-term slip rate, which is also given by numbers in mm/a. Vectors (of constant size) show direction of relative motion of hanging walls. While this is a reasonable approximation of tectonics, table 4 of Bird and Kong (1994) gives more reliable estimates of long-term seismic hazard than this figure. Computed with FAULTS and plotted with Faults2AI.

forces which were found necessary to enforce the velocity boundary conditions on model edges (or subducting slabs). (Currently, SHELLS is the only program which computes boundary nodal forces.)

12. Make as many plots of the output as desired. This step is essentially the same as step #5, except that more output fields are now available.
13. Evaluate the realism of the simulation experiment. The testable predictions of any simulation experiment include:

    - Horizontal velocity vectors, for comparison with relative benchmark velocities determined by geodesy.
    - Azimuths of the most-compressive horizontal principal stress, for comparison with in-situ data, fault plane solutions, dike trends, mesoscale structural analysis, etc.
    - Seafloor spreading rates, for comparison with 3-Ma-average rates determined from maps of marine magnetic anomalies.
    - Seismicity within the surface lithosphere (<70 km depth?) expressed as fault slip and anelastic strain rates. Examine the Fortran 77 code of the scoring program in file OrbScore. Depending on your problem and the datasets available to you, you may be able to use it unchanged (by matching your data format to that of the authors) or you may have to rewrite some of it.

14. Experiment with parameters to reduce prediction errors. See how the quality of the simulation is affected by boundary conditions, fault friction coefficient, mantle flow pattern, fault dips and interconnections, etc.! Use the prediction errors obtained from step (13) as an objective guide as to

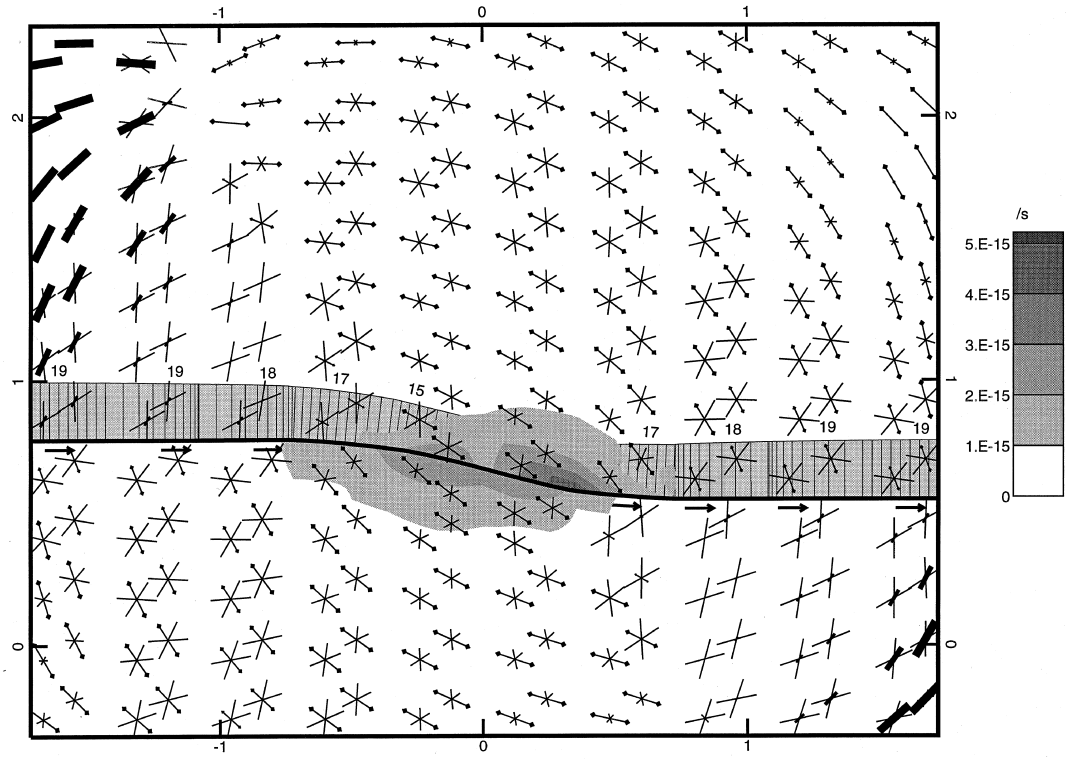

Fig. 5. Continuum strain rate (expressed as microfault orientations) in the vicinity of 25-km right step in vertical strike-slip fault with friction coefficient 0.17. Friction in surrounding blocks is 0.85. Dumbell symbol shows conjugate thrust faulting; X symbol shows conjugate strike-slip faulting; black rectangle shows conjugate normal faulting. All fault symbols are plotted same size for legibility. Magnitude of continuum strain rate is only large near right step, as shown by shaded contours. As in Fig. 4, ribbon symbol shows slip rate of master fault, which decreases smoothly from 20 to 15 mm/a in center of step. Latitudes and longitudes around margin give scale. Computed with PLATES and plotted with Plates2AI.

which model is more realistic and try to minimize the sizes of these various prediction errors. While every model (and every parameter set) contains its own systematic errors with respect to a real planet, we may reasonably hope that when we compare two simulations to see the differential effect of one parameter, that the effect(s) of these systematic errors will largely cancel! In this way, we hope to get reliable insights about real planets from these imperfect models.

5. Model predictions

Fig. 3, 4, 5 and 6 show examples of the four most important types of predictions obtained from any of these models: surface velocity, fault slip rate, continuum strain rate and vertically-integrated stress anomaly.

Surface velocity (Fig. 3) may be compared to relative drift rates obtained from repeated geodetic surveys. Of course, the velocity reference frame is arbitrary and is implicitly defined during the selection of boundary conditions. Because of the neglect of elastic strain in these codes, no velocity perturbations associated with earthquake cycles are included in the predictions. Therefore, predictions may not match geodetic observations taken at benchmarks close to faults which are only temporarily locked. However, this discrepancy can be largely repaired by using a summation of dislocation-patch-in-elastic-halfspace solutions, where the dislocation patches are added to the model to temporarily lock the upper frictional part of each fault element. Examples of such corrections can be found in Bird and Kong (1994) and Bird (1996).

Fault slip rate predictions (Fig. 4) can be plotted either as the slip rate in the fault plane or as its horizontal component, which is the difference in the hori-

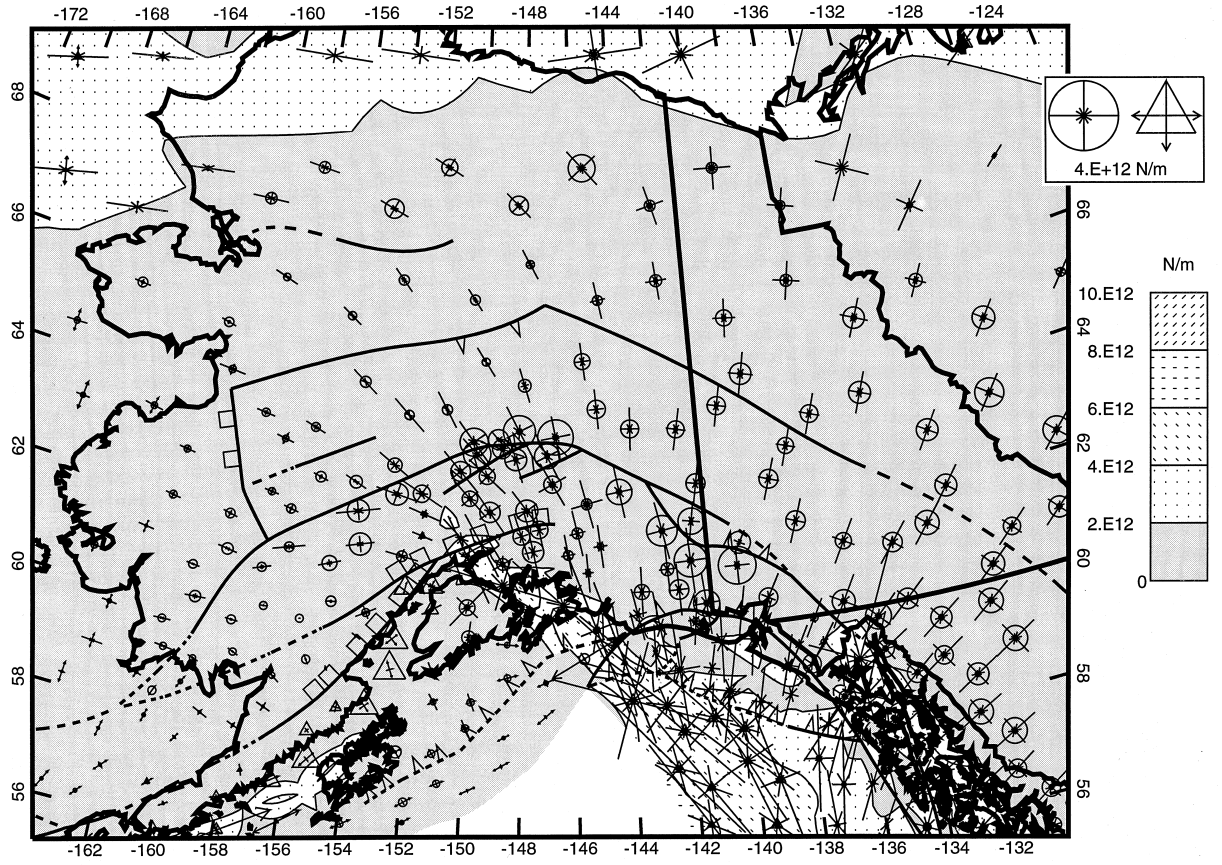

Fig. 6. Vertically-integrated stress anomalies near Alaskan syntaxis from model AK9801, based on AK9549 of Bird (1996). Compression is shown by circles (when vertical) and by converging arrows (when horizontal). Relative tension is shown by triangles and diverging arrows. Shading patterns show vertical integral of greatest shear stress in lithosphere. Faults and coastlines are shown for location reference. Horizontal compression fans out from point where Yakutat terrane is accreting, in good agreement with stress-direction data (Zoback, 1992). Computed with PLATES and plotted with Plates2AI.

zontal velocity vector of the two sides. Faults with non-vertical dips are free to slip parallel to dip, parallel to strike, or obliquely. Faults with vertical dip are constrained to pure strike-slip. Because the blocks on each side of a fault are able to deform internally, fault slip rates will frequently be predicted to change along strike. Because of the neglect of elastic strain in these codes, model faults either lock (permanently) or they slip at a constant rate. The models make no predictions about whether the slip rate on a particular real fault will be expressed aseismically as steady fault 'creep' or seismically as intermittent earthquakes, nor can they make any predictions about how close to failure a particular real fault may be. However, it is reasonable to assume that the long-term seismic hazard from faults is proportional to their long-term slip rates, at least until there is direct evidence of widespread fault creep.

Continuum strain rate (Fig. 5) is defined as the strain rate of the continuum (triangular) elements, without any regard for nearby fault slip. We usually plot this strain rate in terms of the orientations of the conjugate microfaults that would result in a material with the specified coefficient of friction. A general strain rate tensor requires two sets of conjugate faults:

- two orthogonal sets of thrust faults or
- one set of thrust faults and one set of strike-slip faults or
- one set of normal faults and one set of strike-slip faults or
- two orthogonal sets of normal faults.

These predictions are comparable to mesoscale data from structural geology, in which it is common to compile orientations and slip senses of small faults

which are not individually mapable. Also, by mentally connecting together any predicted microfaults of like type, one can roughly envision the map pattern of any new master faults which would form in the future. (Purely plastic thin-sheet codes give such predictions with better precision, but also with less accuracy.)

Stress in the Earth is monotonously compressive and nearly proportional to depth. In order to bring out small variations around this background state, most of the pressure must be subtracted. However, if the actual local pressure is subtracted, then the resulting 'deviatoric stress' does not satisfy the equilibrium equation, nor does it give an intuitive understanding of tectonic mechanisms when it is plotted. Instead, we define a 'stress anomaly' tensor as the total stress tensor minus the isotropic pressure that would be found at the same elevation beneath a mid-ocean spreading ridge. This stress anomaly includes pressure anomalies with sizes comparable to the shear stress components. The stress anomaly also satisfies a modified equilibrium equation (one in which density is replaced by density anomaly). In thin-plate modeling, a natural measure of the stress anomaly distribution is its vertical integral through the strong surface layer: for LARAMY and FAULTS this is the crust; for PLATES and SHELLS it is the whole lithosphere. Vertical integration changes the SI units from Pa to N/m, but it does not change the tensor nature of the quantity. Thus, we determine and plot its principal horizontal axes and the value of its vertical component as one might do for stress. Fig. 6 is an example of such a plot. It can be compared to stress-orientation data like that collected in the World Stress Map project (Zoback, 1992).

Because LARAMY (alone) is a finite-strain program which steps through geologic time, it also yields predictions of the variations of such quantities as:

- Crustal thickness.
- Mantle lithosphere thickness.
- Heat flow.
- Travel–time anomaly for vertically-incident P and S waves.
- Elevation.

Unfortunately, comparable data are usually only available for the present, so one is required to guess the past distributions when initializing the model, and one then hopes roughly to approximate the present distributions at the end of the model (e.g. Bird, 1988, 1992). It is not possible to run LARAMY backwards (with negative time steps) because then the diffusion of heat and the diffusion of crustal thickness would both tend toward spontaneous singularities.

Acknowledgements

These programs were developed by the author over 22 years at UCLA with important assistance from students. John Baumgardner aided in the development of the fault elements for FAULTS which were later adapted for PLATES and SHELLS. Xianghong Kong derived and programmed the complex algebra necessary to create SHELLS, in which stress, strain, stiffness and equilibrium are expressed in spherical coordinates. These programming efforts were supported at various times by the University of California, the National Science Foundation, the US Geological Survey and the National Aeronautics and Space Administration.

References

Bird, P., 1988. Formation of the Rocky Mountains, western United States: a continuum computer model. Science 239 (25 March), 1501–1507.

Bird, P., 1989. New finite element techniques for modeling deformation histories of continents with stratified temperature-dependent rheologies. Journal of Geophysical Research 94 (B4), 3967–3990.

Bird, P., 1992. Deformation and uplift of North America in the Cenozoic era. In: Billingsley, K.R., Brown, H.U., III, Derohanes, E. (Eds.), Scientific Excellence in Supercomputing: the IBM 1990 Contest Prize Papers 1. Baldwin Press, Athens, GA, pp. 67–105.

Bird, P., 1996. Computer simulations of Alaskan neotectonics. Tectonics 15 (2), 235–236.

Bird, P., 1998. Testing hypotheses on plate driving mechanisms with global lithosphere models including topography, thermal structure, and faults. Journal of Geophysical Research 103 (B5), 10.115–10.129.

Bird, P., Kong, X., 1994. Computer simulations of California tectonics confirm very low strength of major faults. Geological Society of America Bulletin 106 (2), 159–174.

Bird, P., Piper, K., 1980. Plane-stress finite-element models of tectonic flow in southern California. Physics of Earth and Planetary Interiors 21, 158–175.

Coblentz, D.D., Richardson, R.M., 1996. Analysis of the South American intraplate stress field. Journal of Geophysical Research 101 (B4), 8643–8658.

England, P.C., Houseman, G.A., 1985. The influence of lithosphere strength heterogeneities on the tectonics of Tibet and surrounding regions. Nature (London) Physical Science 315, 297–301.

England, P.C., Houseman, G., 1986. Finite strain calculations of continental deformation. 2: comparison with the India–Asia collision zone. Journal of Geophysical Research 91 (B3), 3664–3676.

England, P., Houseman, G., 1989. Extension during continental convergence, with application to the Tibetan Plateau. Journal of Geophysical Research 94 (B12), 17.3561–17.579.

England, P., Houseman, G., Sonder, L., 1985. Length scales for continental deformation in convergent, divergent, and strike-slip environments: analytical and approximate sol-

utions for a thin viscous sheet model. Journal of Geophysical Research 90 (B5), 3551–3557.

England, P.C., Searle, M., 1986. The Cretaceous-Tertiary deformation of the Lhasa block and its implications for crustal thickening in Tibet. Tectonics 5 (1), 1–14.

Grindlay, N.R., Fox, P.J., 1993. Lithospheric stresses associated with nontransform offsets of the Mid-Atlantic Ridge: implications from a finite element analysis. Tectonics 12 (4), 982–1003.

Grunthal, G., Stromeyer, S., 1992. The recent crustal stress field in central Europe: trajectories and finite element modeling. Journal of Geophysical Research 97 (B8), 11.805–11.820.

Houseman, G., England, P.C., 1986. Finite strain calculations of continental deformation. 1: method and general results for convergent zones. Journal of Geophysical Research 91 (B3), 3651–3663.

Houseman, G., England, P., 1993. Crustal thickening versus lateral expulsion in the Indian–Asian continental collision. Journal of Geophysical Research 98 (B7), 12.233–12.249.

Kasapoglu, K.E., Toksöz, M.N., 1983. Tectonic consequences of the collision of the Arabian and Eurasian plates: finite element models. Tectonophysics 100 (1/3), 71–95.

Kong, X., 1995. Numerical modeling of the neotectonics of Asia: a new spherical shell finite element method with faults. Ph.D. Dissertation, University of California, Los Angeles, CA, 227 pp.

Kong, X., Bird, P., 1995. SHELLS: a thin-plate program for modeling neotectonics of regional or global lithosphere with faults. Journal of Geophysical Research 100 (B11), 22.129–22.131.

Kong, X., Bird, P., 1996. Neotectonics of Asia: thin-shell finite element models with faults. In: Yin, A., Harrison, T.M. (Eds.), The Tectonic Evolution of Asia. Cambridge University Press, Cambridge, pp. 18–34.

Lundgren, P.R., Russo, R.M., 1996. Finite element modeling of crustal deformation in the North America–Caribbean plate boundary zone. Journal of Geophysical Research 101 (B5), 11.317–11.328.

Peltzer, G., Saucier, F., 1996. Present-day kinematics of Asia derived from geologic slip rates. Journal of Geophysical Research 101 (B12), 27.943–27.956.

Richardson, R.M., 1978. Finite element modeling of stress in the Nazca plate: driving forces and plate boundary earthquakes. Tectonophysics 50, 223–248.

Richardson, R.M., Cox, B.L., 1984. Evolution of oceanic lithosphere: a driving force study of the Nazca plate. Journal of Geophysical Research 89 (B12), 10.043–10.052.

Richardson, R.M., Reding, L.M., 1991. North American plate dynamics. Journal of Geophysical Research 96 (B7), 12.201–12.223.

Richardson, R.M., Solomon, S.C., Sleep, N.H., 1979. Tectonic stress in the plates. Reviews of Geophysics 17 (5), 981–1019.

Solomon, S.C., Richardson, R.M., Bergman, E.A., 1980. Tectonic stress: models and magnitudes. Journal of Geophysical Research 85 (B11), 6086–6092.

Sonder, L.J., England, P.C., Houseman, G.A., 1986. Continuum calculations of continental deformation in transcurrent environments. Journal of Geophysical Research 91 (B5), 4797–4810.

Vilotte, J.P., Daignieres, M., Madariaga, R., 1982. Numerical modeling of intraplate deformation: simple mechanical models of continental collision. Journal of Geophysical Research 87 (B13), 10709–10728.

Vilotte, J.P., Daignieres, M., Madariaga, R., Zienkiewicz, O.C., 1984. The role of a heterogeneous inclusion during continental collision. Physics of Earth and Planetary Interiors 36, 236–259.

Vilotte, J.P., Madariaga, R., Daignieres, M., Zienkiewicz, O.C., 1985. Numerical study of continental collision: influence of buoyancy forces and an initial stiff inclusion. Geophysical Journal of the Royal Astronomical Society 84, 279–310.

Wang, C., Cai, Y., Jones, D.L., 1995. Predicting the area of crustal faulting in the San Francisco Bay region. Geology 23 (9), 771–774.

Wang, K., He, J., Davis, E.E., 1997. Transform push, oblique subduction resistance, and intraplate stress of the Juan de Fuca plate. Journal of Geophysical Research 102 (B1), 661–674.

Zoback, M.L., 1992. First- and second-order patterns of stress in the lithosphere: the World Stress Map project. Journal of Geophysical Research 97 (B8), 11.703–11.728.